INSTITUTE OF PLASMA PHYSICS
CZECHOSLOVAK ACADEMY OF SCIENCES

CALCULATIONS OF SOFT X-RAY EMISSION OF REB-HEATED PLASMA

J. Rauš, V. Babický

RESEARCH REPORT

IPPCZ 287 JANUARY 1989

POD VODÁRENSKOU VĚŽÍ 4, 180 69 PRAGUE 8
CZECHOSLOVAKIA

CALCULATIONS OF SOFT X-RAY EMISSION OF REB-HEATED PLASMA

J. Rauš, V. Babický

IPPCZ 287 January 1989

Abstract

Time dependent spectrum of hydrogen plasma with 1% oxygen impurity in spectral range 5 eV - 5 keV is calculated by using the corona model in the approximation of constant electron temperature (of the order of tens of eV) for interpretation of radiation measurements made on REBEX experiment by means of vacuum X-ray diodes and submicrometer nitrocelulose filters.

1) Introduction

The time dependence of plasma electron temperature on the REBEX experiment (hydrogen plasma of $n_H = 10^{20} - 10^{22}$ m^{-3} heated by relativistic electron beam ~350 kV, 30 kA, 100 ns; resulting Te of tens of eV) is determined from ultrasoft X-ray emission (10 eV - 1 keV) detected by means of vacuum X-ray diodes with Al photocathodes and spectrally analyzed by submicrometer nitrocelulose filters [1]. In the case of hydrogen plasma with impurities, interpretation of results of such measurements by the simple method proposed by Jahoda et al. for the keV spectral region [2] (i.e. determination of Te from the slope of continuum spectra) is possible only in some special cases of REB-plasma interaction regime [3]. In a general case, the whole radiation spectrum of impurities (bremsstrahlung, recombination and line emission) must be taken into account. Therefore, we have calculated the time dependence of emitted spectrum in the range 5 eV - 5 keV, from which theoretical XRD signal and its reduction by filters can be determined.

In this work, which has been made especially to understand the influence of different processes on our measurements, only oxygen impurity is included (for real description of our plasma also nitrogen, carbon and aluminium must be taken into account). For the above mentioned plasma parameters the nonstacionary corona model is used [4] (including electron impact ionization and excitation, spontaneous radiative decay and radiative and dielectronic

recombination) in the approximation of constant electron temperature (which was found to be not too bad in the case of heating by "nanosecond" REB in REBEX experiment).

Soft X-ray emission calculations made for tokamak plasmas are intent on the total radiation losses in steady state [5,6] or on the time dependence of selected spectral lines intensity [7]. The earlier time dependent calculations made in connection with toroidal pinches [8] are uncomplete because of very little data available in that period. Astrophysical works are intent on the detailed spectra calculations in steady state at very low densities [9,10]. In comparison with all these calculations, in our case the time dependence of all the emitted spectra must be determined, but with not very high spectral resolution (with respect to the detection system characteristics). Some special conditions of plasma in a strong ionization nonequilibrum must be taken into account.

Our calculations were made by using the computer SM 52/11 and grafical output of Tektronix 4041 controller.

2) Atomic processes

2.1. Ionization

In the approximation of corona model only electron impact ionization from the ground state is taken into account (ionization by electrons from excited states, photoionization and autoionization are neglected with respect to the low

plasma density). The ionization rate coefficients are given under the assumption of a maxwellian distribution of electron energy; it is established in our plasma within the time of (1 - 100) ns depending especially on n_e (when neglecting a small group of overthermal electrons). For these coefficients for ionization from i-th (sub)shell of ions with charge Q (i=1s,2s,2p) we have used the following formula proposed by Hinnov (taken from ref.[11]):

$$S_i(Q) = 3 \cdot 10^{-14} T_e^{-3/2} \xi_i(Q) \frac{Ei\left(I_i(Q)/T_e\right)}{I_i(Q)/T_e}$$

The total coefficient is $S(Q) = \sum_i S_i(Q)$ (i.e. inner shell ionization is included). Here $S_i(Q)$ are in $m^3 s^{-1}$, Te is the plasma electron temperature in eV, $\xi_i(Q)$ is the number of equivalent electrons in the i-th (sub)shell of ion with charge Q and $I_i(Q)$ is the binding energy of electrons in this (sub)shell (given by Lotz [12]). Ei(x) is the exponential integral

$$Ei(x) = \int_x^\infty \frac{e^{-y}}{y}\, dy$$

which is approximated in the following way [13]:

$$Ei(x) = \frac{e^{-x}}{x}\left(0{,}9999965 - 0{,}9989710\, x^{-1} + 1{,}9487646\, x^{-2} - \right.$$
$$- 4{,}9482092\, x^{-3} + 11{,}7850792\, x^{-4} - 20{,}4523840\, x^{-5} +$$
$$\left. + 21{,}1499469\, x^{-6} - 9{,}5240410\, x^{-7}\right)$$

for x<2, and

$$Ei(x) = -C - \ln x - \sum_{n} (-1)^{n} \frac{x^{n}}{n \cdot n!}$$

with C = 0,5772 (Euler constant) for x>=2.

The needed atomic constants are shown in Tab.1. The Hinnov formula used is equivalent to that proposed by Lotz [14] for Q>=4. In Fig.1 the temperature dependence of $S_{\alpha}(Q)$ (as universal dependence of S/Smax on I/Te) is shown. It reaches a maximum at I/Te ~ 0.1 (the maximum value is Smax = $1{,}7 \cdot 10^{-6} \cdot I^{-3/2}$), followed by a rapid decrease for lower temperatures and relatively low decrease for higher temperatures. It is seen that ionization from the K shell, when the L shell is not fully stripped, is important only for very high temperatures. To acquire the notion of the differences in rate coefficients obtained by different ways, also dependences of $S_{\alpha}(Q)$ calculated by means of the formula used by Post et al.[6] and that proposed by Kolb (published in ref.[4]; it was used in our earlier estimations of ionization state [3]) are shown. These differences are not substantial.

2.2. Electron impact excitation

In our calculations we assume, that the line emission is caused only by optically allowed transitions by spontaneous decay of excited states. Influence of spin-change and forbidden transitions was not studied. Therefore, only the fundamental resonant transitions are taken into account - see Tab.1 (averaged over all terms, when needed). Rate

coefficients for electron impact excitation are calculated as [15] (in $m^3 s^{-1}$)

$$F_j(Q) = 10^{-7} c_j(Q) E_j(Q)^{-3/2} \left(\frac{E_j(Q)}{T_e}\right)^{1/2} e^{-E_j(Q)/T_e}$$

i.e. the temperature dependence is assumed to be universal for all included transitions (in contradiction to ref [16], for example). Here $E_j(Q)$ are energies of the corresponding transitions (in eV) and $c_j(Q)$ are individual constants. These parameters are taken from references [5,15,17] and are given in Tab.1. In Fig.2 the dependence of F/Fmax on E/Te is shown. It is similar to that of ionization rate coefficients with the maximum value F max $=0{,}43.10^{-7}.c.E^{-3/2}$ at E/Te = 0,5.

2.3. Recombination

For plasma parameters corresponding to the corona model, radiative and dielectronic recombination must be taken into account. For the radiative recombination rate coefficients we have modified the standardly used formula [5,11] in the following way:

$$R_{10}(Q) = 9{,}59\cdot 10^{-20} Q^2 T_e^{-3/2} \left(1-\xi_{10}(Q)\right) \frac{I_{10}(Q-1)}{T_e} e^{I_{10}(Q-1)/T_e} E_i\left(I_{10}(Q-1)/T_e\right)$$

$$R_{20}(Q) = 1{,}20\cdot 10^{-20} Q^2 T_e^{-3/2} \left(2-\xi_{20}(Q)\right) \frac{I_{20}(Q-1)}{T_e} e^{I_{20}(Q-1)/T_e} E_i\left(I_{20}(Q-1)/T_e\right)$$

$$R_{21}(Q) = 1{,}20\cdot 10^{-20} Q^2 T_e^{-3/2} \left(6-\xi_{21}(Q)\right) \frac{I_{21}(Q-1)}{T_e} e^{I_{21}(Q-1)/T_e} E_i\left(I_{21}(Q-1)/T_e\right)$$

$$R_{3s}(Q) = 1{,}92\cdot10^{-11}\, Q^2 T_e^{-3/2} \sum_{n=4}^{15} \frac{1}{n^3} \frac{I_n(Q-1)}{T_e}\, e^{I_n(Q-1)/T_e}\, E_1\left(I_n(Q-1)/T_e\right)$$

where R1s(Q), R2s(Q) and R2p(Q) (in $m^3 s^{-1}$) describe recombination of ion with charge Q to the corresponding (sub)shell, the term $(k_i - \xi_i(Q))$ is the number of empty places in this shell. R3 represents recombination in excited levels with principal quantum number n>=3, which are assumed to be hydrogenic (i.e. $I_n(Q-1) = 13{,}6\ eV \times Q^2/n^2$) Binding energies of electrons in subshells 2s and 2p in the cases when these levels are fully stripped (in parentheses in Tab.1), are determined as the difference between binding energy in the valence shell of ground state and excitation energy of the respective levels. This modification of formula for $R_i(Q)$ is suitable because of its applicability also to the calculation of radiation spectrum.

In Fig.3 the universal temperature dependence of $R_i(Q)$ (i.e. R/Rmax on I/Te) is shown. Rmax in this case (the curve shows monotonous increase) is the maximum in the figure, i.e. at I/Te = 100. Fig.4 shows the dependence of R on the principal quantum number (in the form Q/n) for different temperatures, from which necessary number of terms in summation for calculation of R3 can be determined; we use summation up to n = 15 (see equations for R (Q); for comparison, in ref [18] summation up to n = 10 was used)

Dielectronic recombination rate coefficients for oxygen are calculated using the formula proposed by Vainshtein [19] in the following form (in $m^3 s^{-1}$)

$$K_j(Q) = 10^{-14}\, d_j(Q)\left(\frac{E_j(Q)}{T_e}\right)^{3/2} e^{-E_j(Q)/T_e}$$

where $K_j(Q)$ is the rate coefficient for dielectronic recombination of an ion with charge Q by excitation of its j-th resonant transition of energy $E_j(Q)$, and $d_j(Q)$ are individual constants. For Q = 1..3, the transitions (2s-2p) and (2p-3d), for Q = 4 and Q = 5 (2s-2p) and (2s-3p), while for Q = 6 and Q = 7 only the first resonant transition (1s-2p) are taken into account.

The needed constants $d_j(Q)$ (as given in the book by Presnyakov et al.[20]) and transition energies are given in Tab.1. Temperature dependence of coefficient K (K/Kmax on E/Te) is shown in Fig.5; dielectronic recombination is a strongly resonant process with the maximum probability at E/Te = 1,5 and maximum coefficient value $Kmax = 0{,}4.10^{-14}.d$.

In the first approximation, density dependence of dielectronic recombination is neglected. Since it can partially influence the ionization state at our densities [6], in the planned more precise calculations it must be taken into account.

The total recombination rate coefficient of ions with charge Q in our calculations is given by

$$\beta(Q) = [K_1(Q) + K_2(Q)] + [R_{1s}(Q) + R_{2s}(Q) + R_{2p}(Q) + R_3(Q)] = K(Q) + R(Q).$$

3) Ionization state of impurities

Plasma on the REBEX machine is generated by plasma guns,

the electric discharge in hydrogen gas starting on the surface of guns insulators. Plasma density is varied between 10^{20} and 10^{22} m^{-3} by changing the hydrogen pressure and gun parameters. Temperature of such a plasma has been determined to be of several eV (~3eV). Impurities come into the plasma especially from the guns insulators surfaces, i.e. principal impurities are the light elements C,N,O and Al, which can be partially deposited on these surfaces from the anode foil of REB generator. Typical density of these impurities estimated from the magnitude of XRD signals is 10^{19} m^{-3}, i.e ~1% of n_e [3]. This plasma is heated by REB (~350 kV, 30 kA, 100 ns), the injection time of which is much shorter then the lifetime of hot plasma (1 - 4 μs for different regimes) and characteristic ionization times of impurities. Relaxation of overthermal electrons (caused by REB-plasma interaction) and dissipation of energy of redistributed magnetic field can cause, in some regimes, mild additional heating of plasma after REB injection [21]. Therefore, in the first approximation, we have assumed the following model:

Hydrogen plasma of $n_e = 10^{20} - 10^{22}$ m^{-3} with 1% oxygen impurity in ionization state O^{4+} (approximately corresponding to the forplasma Te) is heated at instant $t = 0$ to Te of several tens of eV, which is than conserved. With this assumption, the time dependence of densities of oxygen in higher ionization states is determined.

The differential equations describing the ionization state of oxygen are:

$$\frac{dn(Q)}{d\lambda} = -n(Q)\,n_e\,S(Q,T_e) + n(Q+1)\,n_e\,\beta(Q+1,T_e) \qquad Q=0$$

$$\frac{dn(Q)}{d\lambda} = -n(Q)\,n_e\,[S(Q,T_e)+\beta(Q,T_e)] + n(Q-1)\,n_e\,S(Q-1,T_e) + n(Q+1)\,n_e\,\beta(Q+1,T_e) \qquad Q=1\div7$$

$$\frac{dn(Q)}{d\lambda} = -n(8)\,n_e\,\beta(Q,T_e) + n(Q-1)\,n_e\,S(Q-1,T_e) \qquad Q=8$$

with initial conditions based on our assumptions

$$n(1)_{\lambda=0} = 1 \quad , \quad n(Q+1)_{\lambda=0} = 0$$

Here n(Q) is the relative density of oxygen ions with charge Q (in comparison to the total oxygen density), S(Q,Te) and β(Q,Te) are, respectively, ionization and recombination rate coefficients at the electron temperature Te.

In the case of ionization equilibrium, the relative densities φ(Q) are given by

$$\frac{\varphi(Q)}{\varphi(Q+1)} = \frac{\beta(Q+1,T_e)}{S(Q,T_e)} \quad , \quad \sum_{Q=0}^{8}\varphi(Q) = 1$$

In our calculations, the above mentioned differential equations are solved numerically by the Euler method on the assumption of constant Te (i.e. constant coefficients S and β). Analytical solutions are obtainable only in some special cases:

a) Solutions published in ref.[22] are made for the constant Te on the assumption that during the time period that n(Q) is varying rapidly, only the adjacent states, Q-1 and Q+1, have a time varying population, all states lower than Q-1

having reached a steady state and all states higher than Q+1 having yet to be populated. In our case, this assupmtion is not satisfied. This fact was confirmed also by the comparison of results obtained by numerical and this analytical solutions.

b) In the case when ionization is the dominating process and recombination can be neglected, equation similar to that used for chain radioactive decay can be used [4] (also only at constant Te). Results obtained from this equation are similar to those of numerical calculations in our case, especially in shorter time intervals. Therefore, for estimation of ionization state the times of maximum density of individual ionization stages, obtained by derivative of this equation, can be used:

$$\tau(Q) = \frac{1}{n_e [S(Q-1) - S(Q)]} \ln \frac{S(Q-1)\,[S(Q-2) - S(Q)]}{S(Q)\,[S(Q-2) - S(Q-1)]}$$

Time dependent relative densities of oxygen ions with charge Q = 1..8 at different electron temperatures obtained in our numerical calculations are shown in Fig.6 - 10 (dependence on the product $n_e.t$ is universal for all densities). These results confirm the strong ionization nonequilibrum of our plasma. For comparison, we have calculated also the distribution of ionization stages of oxygen in corona equilibrum in dependence on Te. Results, shown in Fig.11, are in reasonable agreement with those of other authors [5,6].

4) Soft X-ray emission

4.1. Continuum

The continuum spectrum of plasma radiation includes bremsstrahlung and continuous part of radiation caused by radiative recombination.

Bremsstrahlung spectrum in our case (i.e. hydrogen plasma with oxygen impurity) is given by

$$P_B(E) = 1{,}5 \cdot 10^{-38}\, T_e^{-1/2}\, g\, e^{-E/T_e}\, n_e \left(n_H + n_O \sum_1^8 Q^2 n(Q) \right)$$

where $P_B(E)$ is the spectral density of radiation intensity of plasma volume 1 m^3 at the energy E (in $W.m^{-3}.eV^{-1}$), n_H is hydrogen density (we have assumed $n_H = n_e$) and n_O is oxygen density. All other symbols have been defined above. Calculations were made under the assumption that the Gaunt factor for bremsstrahlung is equal to 1 for our plasma parameters [23].

Recombination continuum has a similar form as bremsstrahlung spectrum (i.e. exponential slope), but with thresholds at energies corresponding to the ionization potentials of the ions after recombination from the (sub)shells, to which electrons were captured. Spectral density of radiation intensity for this case can be written as

$$P_R(E) = \sum_{Q=1}^{8} \sum_i P_{RQi}(E) \quad , \quad i = 1_s, 2_s, 2_p, 3$$

$$P_{RQi}(E) = 0 \quad , \quad E < I_i(Q-1)$$

$$P_{RR,i}(E) = 1.6 \cdot 10^{-14} \frac{R_i(Q,T_e)}{E_i(I_i(Q-1)/T_e)} e^{-E/T_e} n_e n_0 n(Q), \quad E \geq I_i(Q-1)$$

where i are the (sub)shells of the ion after recombination. Spectrum for electron capture to the shells with quantum numbers n>=3 was approximated under the assumption, that all electrons were captured to the shell n = 3, i.e. $I_3(Q-1) = 13.6 \cdot Q^2/9$ (see the recombination rate coefficients). The Gaunt factor for radiative recombination was taken equal to 1 [23]

4.2.Line emission

Line emission is caused by spontaneous decay of excited states, which are produced by electron impact and by both radiative and dielectronic recombination. In the case of dielectronic recombination, the resulting ion is twice excited (the electron is captured to the level with high quantum number with excitation of the resonant transition of an ion before recombination). Energy of the resonant transition is assumed to be not influenced by the outer electron (its decay time is shorter than that for outer electron). The cascade decay of outer electron is approximated by emission of energy of the transition E_{ik} of an ion after recombination, similarly as in the case of radiative recombination to the shells n>=3. This approximation is not fully correct. In Tab.2 all the rate coefficients are shown, as calculated for the typical temperature Te = 50 eV. It is seen, that the part of line emission caused by

recombination plays a substantial role only for oxygen ions with Q = 6..8, which are practically not present in our plasma (as well seen from the time dependence of n(Q)). Therefore, this approximation was find to be good for plasma in REBEX machine. Excitation of level 2p by radiative recombination is also taken into account, when the level 1s is partially or fully stripped. Since we include in our calculations only optically allowed transitions, excitation of level 2s by recombination is not taken into account. On these assumptions, intensities of individual lines can be calculated in the following way:

$$P_{LQ1} = 1{,}6\cdot10^{-19} n_e n_0 \, n(Q)\left(F_1(Q)+K_1(Q)\right)E_1(Q) \quad ; \qquad Q = 1 \div 3$$

$$P_{LQ1} = 1{,}6\cdot10^{-19} n_e n_0 \left[n(Q)\left(F_1(Q)+K_1(Q)\right)+n(Q+1)R_{21}(Q+1)\right]E_1(Q) \quad ; \qquad Q = 4 \div 7$$

$$P_{LQ2} = 1{,}6\cdot10^{-19} n_e n_0 \left[n(Q)\left(F_2(Q)+K_2(Q)\right)+n(Q+1)\left(K(Q)+R_2(Q)\right)\right]E_2(Q)$$

$$P_{LQ3} = 1{,}6\cdot10^{-19} n_e n_0 \, n(Q)F_3(Q)E_3(Q)$$

where P_{LQj} (in $W.m^{-3}$) is the intensity of j-th resonant line of ion with charge Q emitted from the plasma volume of 1 m^3.

4.3. Calculation of spectrum

The spectrum is calculated as the spectral density of radiative power in the spectral range of 5 eV -5 keV in 180 points (i.e 60 points within one order of energies). Within the intervals between two points it is assumed to be constant (the relative width of intervals is $E/\Delta E \sim 26$).

Since the only time dependent terms in equations for spectrum calculation are the relative oxygen densities n(O), we calculate the "universal spectrum" for individual temperatures (for $n_e = 0{,}01\ n_H$; the symbols PP are the density independent intensities $P/n_H/n_e$) in the following form:

hydrogen bremsstrahlung:

$$PP_H(E) = 1{,}5 \cdot 10^{-36}\ T_e^{-1/2}\ e^{-E/T_e}$$

oxygen bremsstrahlung:

$$PP_{BQ}(E) = 1{,}5 \cdot 10^{-38}\ Q^2\ T_e^{-1/2}\ e^{-E/T_e} \quad ; \quad Q = 1 \div 8$$

recombination continuum:

$$PP_{RQ}(E) = \sum_i PP_{RQ_i}(E) \quad ; \quad i = 1_s, 2_s, 2_p, 3$$

$$PP_{RQ_i}(E) = 0 \quad , \quad E < I_i(Q-1)$$

$$PP_{RQ_i}(E) = 1{,}6 \cdot 10^{-19}\ \frac{R_i(Q,T_e)}{E_i\left(I_i(Q-1)/T_e\right)}\ e^{-E/T_e} \quad ; \quad E \geq I_i(Q-1) \quad ; \quad Q = 1 \div 8$$

line emission:

$$PP_{LQ}(E) = \sum_{j=1}^{5} PP_{LQ_j}(E)$$

where $PP_{LQ_j}(E) \neq 0$ only in the following cases:

$$E_1(Q) \in \Delta E \quad , \quad Q = 1 \div 7 \quad \Rightarrow$$

$$PP_{LQ_1}(E) = 1{,}6 \cdot 10^{-19}\ \left(F_1(Q,T_e) + K_1(Q,T_e)\right)\ \frac{E_1(Q)}{\Delta E}$$

$$E_2(Q) \in \Delta E \quad , \quad Q = 1 \div 7 \quad \Rightarrow$$

$$PP_{LQ_2}(E) = 1{,}6 \cdot 10^{-19}\ \left(F_2(Q,T_e) + K_2(Q,T_e)\right)\ \frac{E_2(Q)}{\Delta E}$$

$$E_3(Q) \in \Delta E \quad , \quad Q = 6;7 \quad \Rightarrow$$

$$PP_{LQ_3}(E) = 1{,}6 \cdot 10^{-19}\ F_3(Q,T_e)\ \frac{E_3(Q)}{\Delta E}$$

$$E_1(Q-1) \leq \Delta E \;,\; Q = 5 \div 8 \Rightarrow$$

$$PP_{LQ4}(E) = 1{,}6 \cdot 10^{-19} R_{24}(Q,T_e) \frac{E_1(Q-1)}{\Delta E}$$

$$E_2(Q-1) \leq \Delta E \;,\; Q = 2 \div 8 \Rightarrow$$

$$PP_{LQ5}(E) = 1{,}6 \cdot 10^{-19} \left(K(Q,T_e) + R_3(Q,T_e)\right) \frac{E_2(Q-1)}{\Delta E}$$

The total spectral density of radiation power (in $W.m^3$ /eV) at the time t (in the density universal form $n_e.t$) is than given by:

$$PP_E(n_e.t) = PP_H(E) + \sum_{Q=1}^{8} \left[PP_{BQ}(E) + PP_{RQ}(E) + PP_{LQ}(E)\right] n(Q; n_e.t)$$

The real intensities emitted by the plasma volume of 1 m^3 can be determined as

$$P_E = n_e n_0 PP_E = 10^{-2} n_e^2 PP_E$$

Examples of calculated spectra are given in Fig.12 - 15. It is seen that recombination thresholds are partially masked by hydrogen bremsstrahlung (especially in shorter time intervals) and that the radiation spectrum is shifted to the higher energies in longer time intervals. The total intensity of continuum is not higher then 1% of the intensity of emitted lines.

For comparison we have calculated also the radiation losses caused by different mechanisms for oxygen in corona equilibrium by using the integrals of different parts of spectrum calculated by the described procedure. Results shown in Fig.16 are in reasonable agreement with those published by other authors [5,6].

5) XRD signals

5.1. Calculated signals

Signals of bare vacuum photodiode with Al photocathode and those of the same detectors with nitrocelulose filters of submicrometer thicknesses are calculated from the time dependent spectrum as

$$I(n_i,h) = \int_{5eV}^{5keV} d\omega(E)\, PP_E(n_i,h)\, dE$$

The sensitivities of detectors $d\omega$ used (in A/W) are shown in Fig.17. The sensitivity of aluminium for E > 10 eV is taken from ref. [24,25], for E < 10 eV it was obtained by extrapolation (the fact that the threshold of sensititvity is at E = 4,26 eV was taken into account). Absorption characteristics of nitrocelulose ($C_6H_8N_2O_9$) for E > 30 eV were obtained from data published by Henke [26] , for 15 eV < E < 40 eV calibration were made by synchrotron radiation in the Institute of Nuclear Physics in Novosibirsk (USSR) and for E < 15 eV the data were obtained by extrapolation.

Signals obtained by this way are density independent (in Am^3). Real signals (in volts) can be determined as

$$U(h) = 10^{-2}\, n_i^2 \cdot V \cdot \Omega \cdot Z \cdot I(h)$$

where V (in m^3) is the viewed plasma volume, $\Omega = S/4\pi R^2$ (S is the photocathode area, R is the distance between detector and plasma) and Z (in ohms) the detector impedance. (In our concrete conditions, the product $V.\Omega.Z \sim 10^{-6}$ m^3.ohm).

In Fig.18 - 22 the signals of bare XRD (I_0) for several temperatures are shown together with respective ratios of signals with filters of typical thicknesses 0,1; 0,25; 0,5 and 0,85 μm to those of bare XRD (I/I_0). It is seen that the ratios corresponding to filter thickness of 0,1 μm are very similar for all included temperatures (in the limit of measurement precision). Information on Te can be obtained only by thicker filters. Some information can be obtained also from the characteristic form of bare XRD signal (especially in the case when n_e is determined in on independent way).

5.2. Comparison with experiment

In Fig.23 the signal of bare XRD is shown, as obtained in one of typical regimes of REB-plasma interaction. It differs from that calculated for Te = 50 eV (Fig.20a) at typical density $n_e = 10^{24}$ m^{-3} only in the front (initial increse caused by plasma heating by REB) and in some quicker decrease at times > 1 μs, which is connected with a hot plasma decay.

Typical results of measurements with filters are shown in Fig.24. In this concrete case, filters of thicknesses 0,09; 0,2; and 0,57 μm were used. Signal with filter 0,57 μm was too small to be registrated. In Fig.25 theoretical ratios I/I_0 are shown for these filter thicknesses for Te = 50 eV ($n_e \sim 10^{24}$ m^{-3} was obtained from the frequency of diamagnetic signal). It is seen that experimental and theoretical ratio

values are in reasonable agreement at t = 1 μs. In shorter time intervals, the ratios obtained with thicker filters are too high. This effect is probably caused by overthermal electrons generated during beam-plasma interaction, which can effectively excite K-lines of low-ionized ions.

6) Conclusion

The model described is suitable for plasma heating by "nanosecond" REB. For better description of processes in such a plasma we plan to include in our calculations other impurities (especially carbon and aluminium) and the influence of overthermal electrons (for example by introducing two-temperature distribution of electron energies). Influence of spin-change and forbidden transitions on line emission and more detailed description of cascade decay of electrons from high principal quantum number levels will be also studied.

For interpretation of planned measurements on experiment with "microsecond" REB (device GOL-3, INP Novosibirsk, REB of ~ 5 μs), where the injection time will be comparable with the plasma lifetime and ionization times, calculations with time dependent electron temperature must be made. These calculations will be difficult because of substantially larger computer time needed (one run several hours on SM 52/11 computer).

7) Acknowledgements

We would like to acknowledge Dr. P. Sunka and Dr. V. Piffl for many helpful discussions.

8) References

[1] Rauš J., Piffl V.: Czech.J.Phys. B38, 11(1988), 1222

[2] Jahoda F.C. et al.: Phys.Rev. 119, 3(1960), 843

[3] Rauš J., Piffl V.: Preprint IPPCZ 278, September 1987 (Institute of Plasma Physics, Prague)

[4] Mc Whinter R.W.P.: in Plasma Diagnostic Techniques, ed. R.H.Huddlestone, S.L.Leonard, Russian translation, Mir, Moscow 1967, 165

[5] Breton C. et al.: J.Quant.Spectr.Rad.Transfer 19(1978), 367

[6] Post D.E.et al.: At.Data Nucl.Data Tables 20,5(1977)397

[7] EQUIPE TFR: Nucl.Fusion 15(1975), 1053

[8] Hobbs G.D. et al.: Proc. 5-th ICPIG (Munich 1961), Amsterodam 1962, Vol.2, 1965

[9] Jordan C.: Mon.Not.R.Astron.Soc. 142(1969), 501

[10] Tucker W.H., Koren M.: Astrophys.J. 168(1971), 283

[11] von Goeler S. et al.: Nucl.Fusion 15(1975), 301

[12] Lotz W.: J.Opt.Soc.Am. 58(1968), 915

[13] Janke E. et al.: Tafeln Hoeherer Funktionen, Russian translation, Nauka, Moscow 1964

[14] Lotz W.: Preprint IPP 1/62, May 1967 (Institut fur Plasmaphysik, Garching)

[15] Tazima T. et al.: Nucl. Fusion 17(1977), 419

[16] Vainshtein L.A. et al.: Secheniya vozbuzhdeniya atomov i ionov elektronami, Nauka, Moscow 1973

[17] Striganov A.R., Odincova G.A.: Tablici spektralnych linij atomov i ionov, Energoizdat, Moscow 1982

[18] Spitzer L.Jr.: Astrophys.J. 107(1948), 6

[19] Vainshtein L.A.: Trudy FIAN 119, Nauka, Moscow 1980, 3

[20] Presnyakov L.P. et al.: Elementarnye procesy s uchastiem mnogozaryadnych ionov, Energoatomizdat, Moscow 1986

[21] Šunka P.: Proc. 16th ICPIG, Duesseldorf 1983, Inv.Pap., 232

[22] Burton W.M., Wilson R.: Proc.phys.Soc.(London) 78(1961), 1416

[23] Lukyanov S.Yu.: Goryachaya plazma i upravlyaemyj yadernyj sintez, Nauka, Moscow 1975

[24] Day R.H.: AIP Conf.Proc. No.75 on Low Energy X-ray Diagnostics, Monterey, California, ed. D.T.Attwood, B.L.Henke (AIP, New York 1981), 44

[25] Day R.H. et al.: J.Appl.Phys 52,11(1981), 6965

[26] Henke B.L.: At.Data Nucl.Data Tables 27,1(1982), 1

Q	1	2	3	4	5	6	7
1s	2,0	2,0	2,0	2,0	2,0	2,0	1,0
2s	2,0	2,0	2,0	2,0	1,0	0,0	0,0
3s	3,0	2,0	1,0	0,0	0,0	0,0	0,0
I1s	565,0	592,0	618,0	645,0	671,0	739,0	871,0
I2s	42,6	63,8	87,6	114,0	138,0	(173,0)	(221,0)
I2p	35,1	54,9	77,4	(94,3)	(126,0)	(165,0)	(221,0)
tr.	2s-2p	2s-2p	2s-2p	2s-2p	2s-2p	1s-2p	1s-2p
E1	14,9	18,5	19,0	19,7	12,0	574,0	650,0
c1	6,24	6,76	8,00	7,69	2,84	3,02	1,83
d1	2,99	6,89	12,6	21,9	12,8	0,54	0,48
tr	2p-3d	2p-3d	2p-3d	2s-3p	2s-3p	1s-3p	1s-3p
E2	28,8	40,7	52,0	72,0	82,6	665,0	775,0
c2	1,39	2,48	0,0	2,57	1,15	2,45	1,40
d2	0,10	0,41	0,76	0,23	0,26	0,0	0,0
tr.						1s-4p	1s-4p
E3						698,0	815,0
c3						2,45	1,40

Tab.1: Atomic constants of oxygen

Tab.2: Rate coefficients, Te = 50 [eV]

Q:	0	1	2	3	4	5	6	7	8
S1s:	2.87E-21	1.52E-21	8.09E-22	4.43E-22	2.38E-22	1.31E-22	2.78E-23	7.21E-25	0.00E+00
S2s:	1.44E-14	5.64E-15	1.87E-15	6.71E-16	2.49E-16	5.46E-17	0.00E+00	0.00E+00	0.00E+00
S2p:	1.22E-13	1.35E-14	2.88E-15	5.11E-16	0.00E+00	0.00E+00	0.00E+00	0.00E+00	0.00E+00
S:	1.37E-13	1.91E-14	4.75E-15	1.18E-15	2.49E-16	5.46E-17	2.78E-23	7.21E-25	0.00E+00
R1s:	0.00E+00	0.00E+00	0.00E+00	0.00E+00	0.00E+00	0.00E+00	0.00E+00	6.25E-19	1.65E-18
R2s:	0.00E+00	0.00E+00	0.00E+00	0.00E+00	0.00E+00	3.16E-20	9.46E-20	1.34E-19	1.82E-19
R2p:	0.00E+00	1.78E-21	1.43E-20	4.69E-20	1.10E-19	1.81E-19	2.79E-19	3.99E-19	5.46E-19
R3:	0.00E+00	1.99E-21	2.10E-20	7.79E-20	1.90E-19	3.72E-19	6.33E-19	9.80E-19	1.42E-18
R:	0.00E+00	3.77E-21	3.53E-20	1.25E-19	3.01E-19	5.85E-19	1.01E-18	2.14E-18	3.79E-18
K1:	0.00E+00	3.61E-18	1.07E-17	2.02E-17	3.65E-17	1.18E-17	2.17E-21	5.09E-22	0.00E+00
K2:	0.00E+00	2.46E-19	1.33E-18	2.85E-18	9.42E-19	1.06E-18	0.00E+00	0.00E+00	0.00E+00
K:	0.00E+00	3.86E-18	1.20E-17	2.30E-17	3.75E-17	1.29E-17	2.17E-21	5.09E-22	0.00E+00
F1:	0.00E+00	2.59E-14	2.34E-14	2.71E-14	2.52E-14	1.39E-14	2.81E-20	3.50E-21	0.00E+00
F2:	0.00E+00	3.14E-15	3.72E-15	0.00E+00	1.55E-15	5.24E-16	3.44E-21	2.02E-22	0.00E+00
F3:	0.00E+00	0.00E+00	0.00E+00	0.00E+00	0.00E+00	0.00E+00	1.73E-21	8.83E-23	0.00E+00

Fig.1

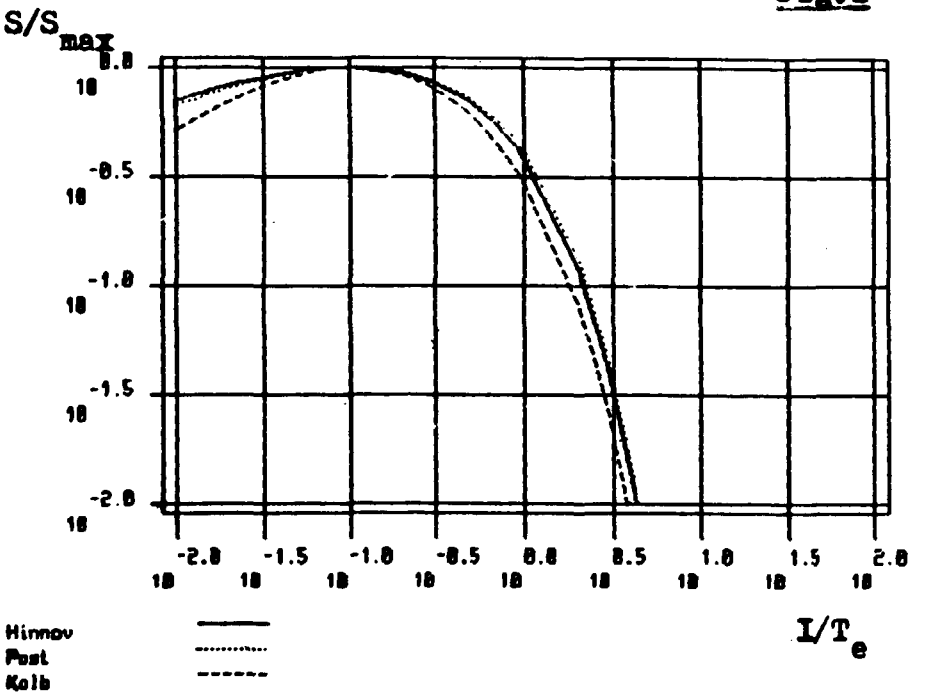
S/S max
0.0
10
-0.5
10
-1.0
10
-1.5
10
-2.0
10
-2.0 -1.5 -1.0 -0.5 0.0 0.5 1.0 1.5 2.0
10 10 10 10 10 10 10 10 10
I/T e
Hinnov
Post
Kolb

Fig.2

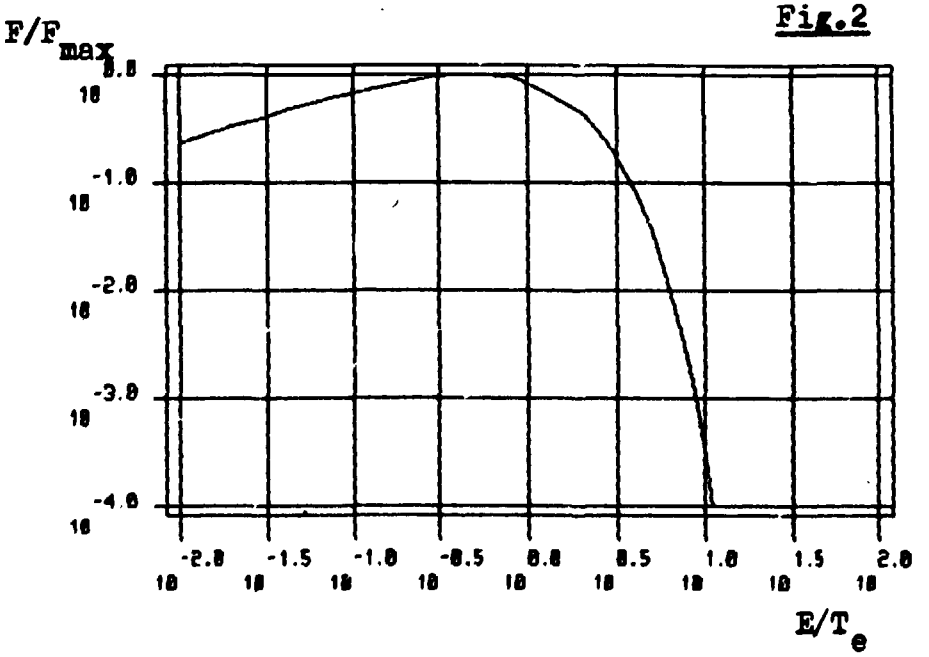
F/F max
0.0
10
-1.0
10
-2.0
10
-3.0
10
-4.0
10
-2.0 -1.5 -1.0 -0.5 0.0 0.5 1.0 1.5 2.0
10 10 10 10 10 10 10 10 10
E/T e

Fig.3

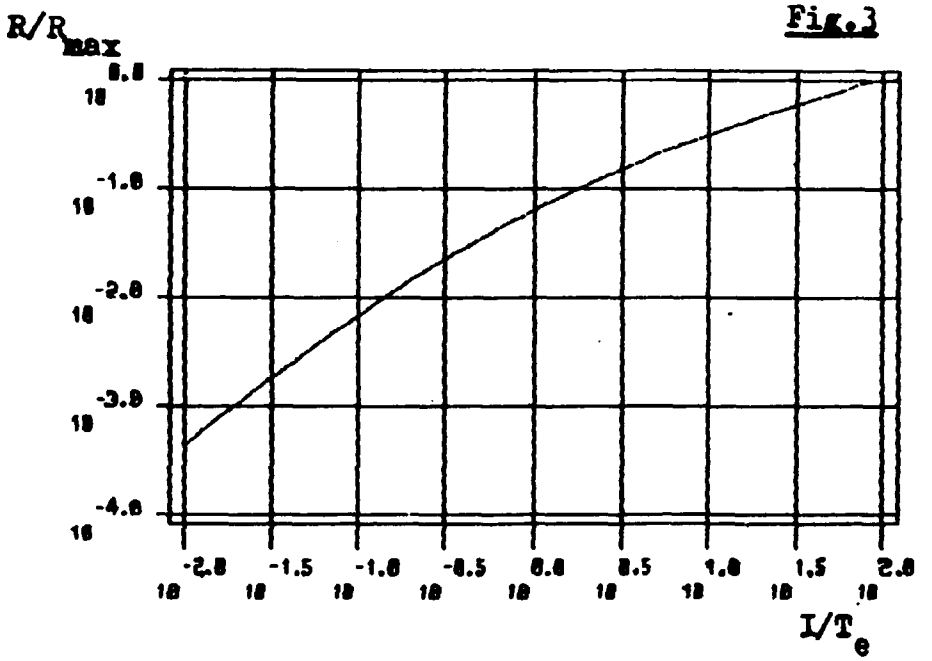

Fig.4

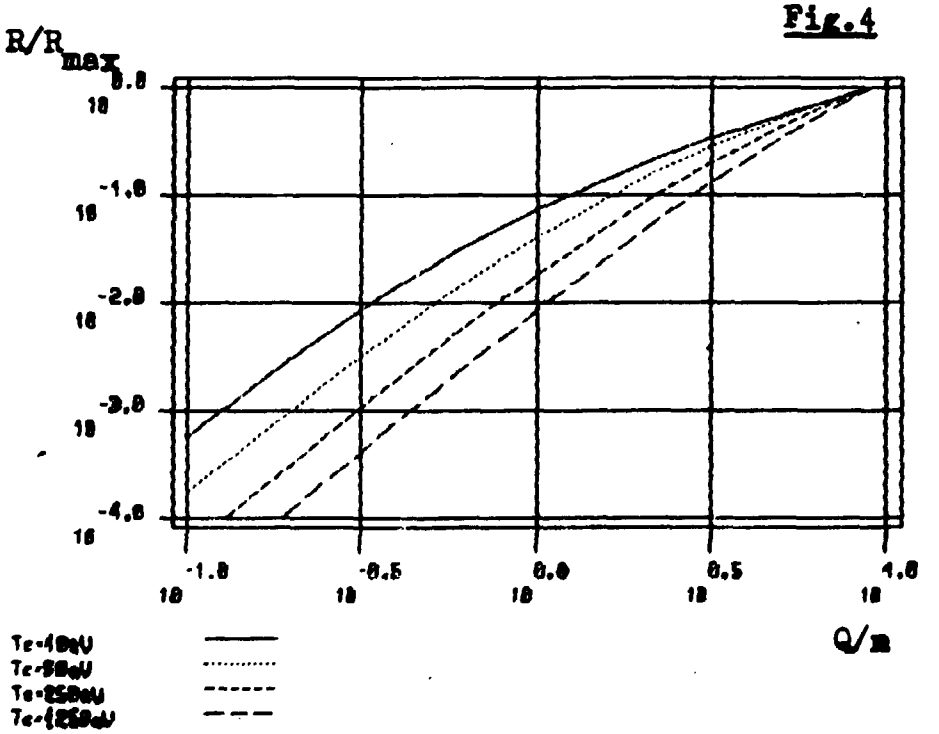

Fig.5

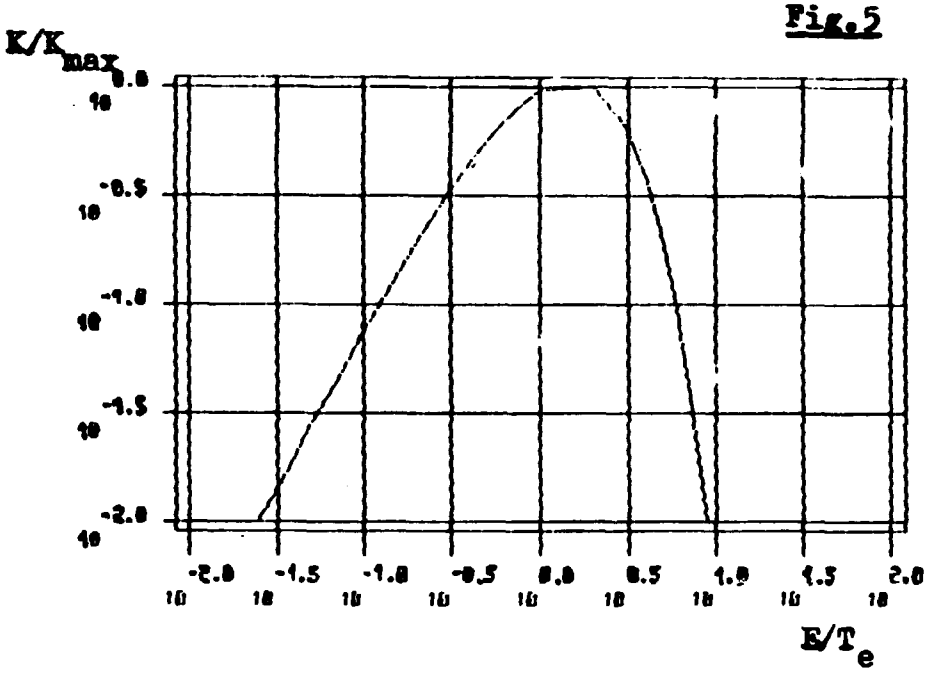

Fig.6

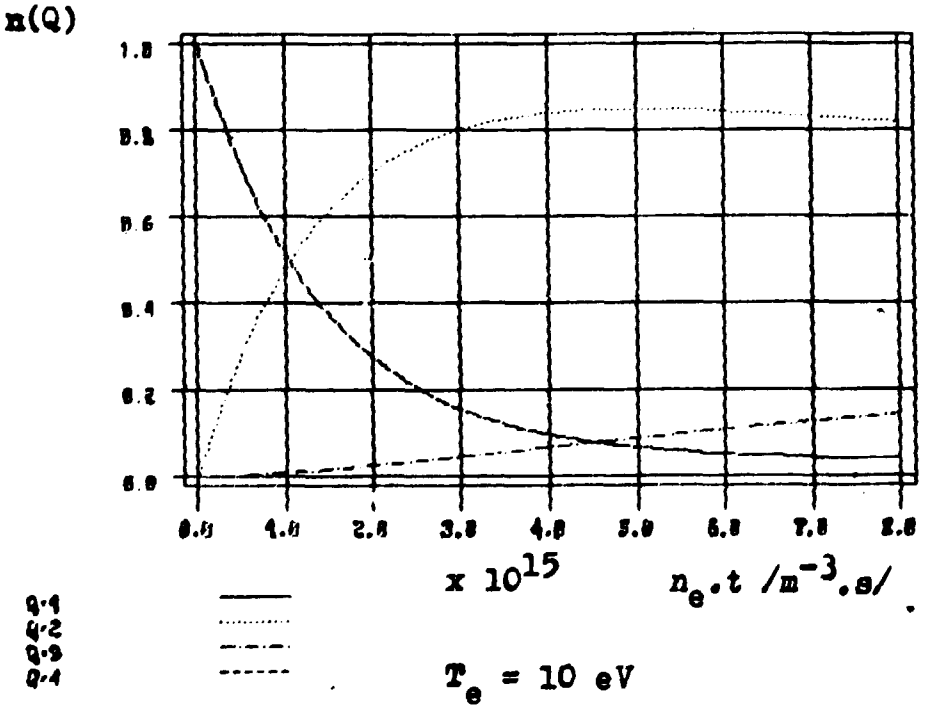

Fig.7a

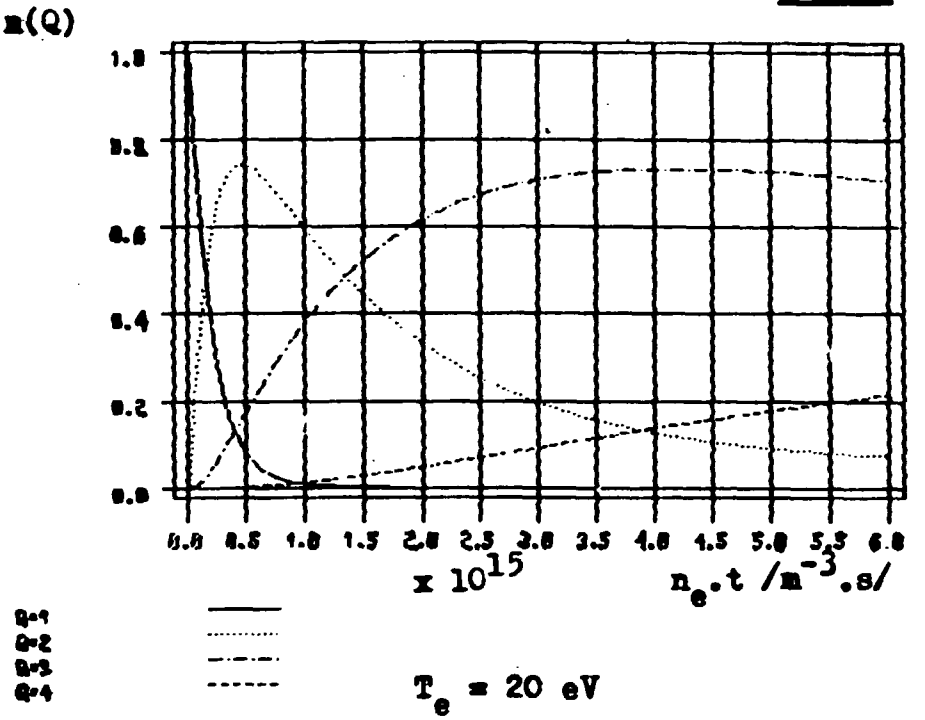
n(Q)
1.0
0.8
0.6
0.4
0.2
0.0
0.0 0.5 1.0 1.5 2.0 2.5 3.0 3.5 4.0 4.5 5.0 5.5 6.0
x 10^15
n_e.t /m^-3.s/
Q=1
Q=2
Q=3
Q=4
T_e = 20 eV

Fig.7b

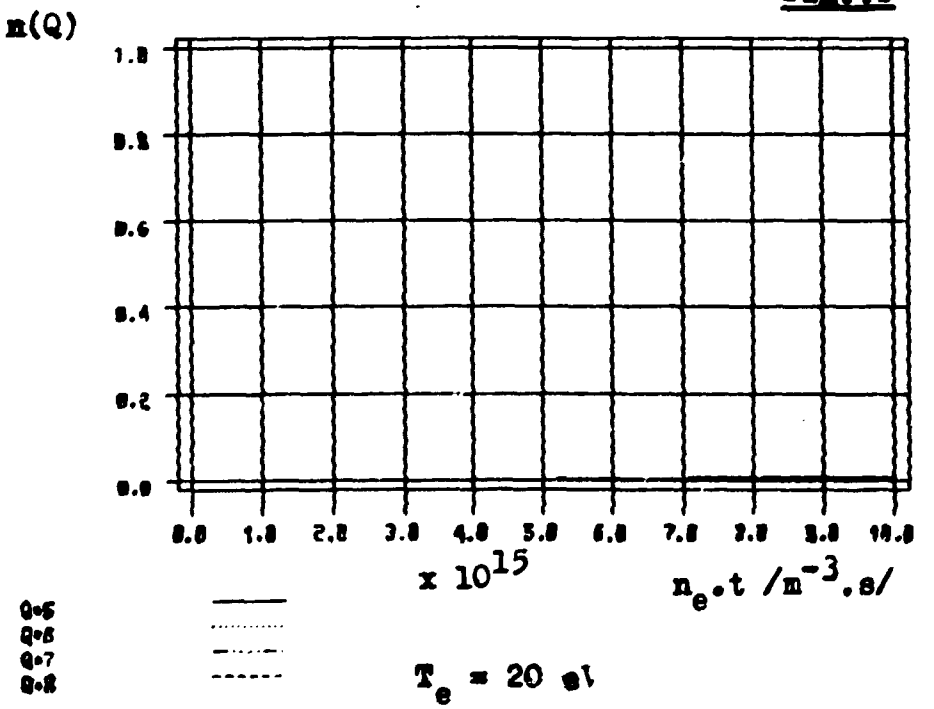
n(Q)
1.0
0.8
0.6
0.4
0.2
0.0
0.0 1.0 2.0 3.0 4.0 5.0 6.0 7.0 8.0 9.0 10.0
x 10^15
n_e.t /m^-3.s/
Q=5
Q=6
Q=7
Q=8
T_e = 20 eV

Fig.8a

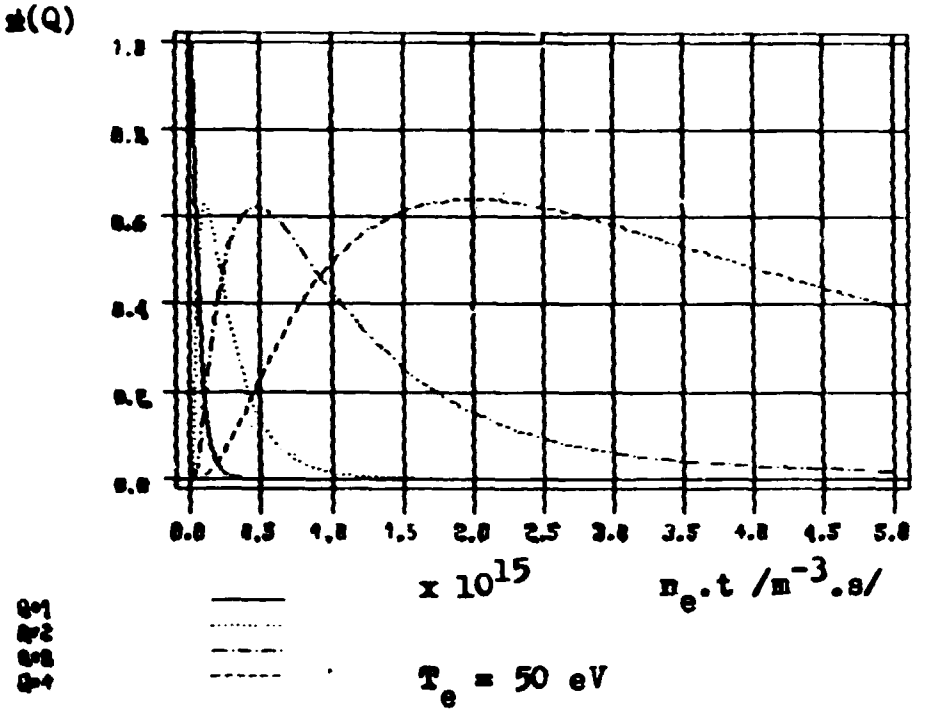

Fig.8b

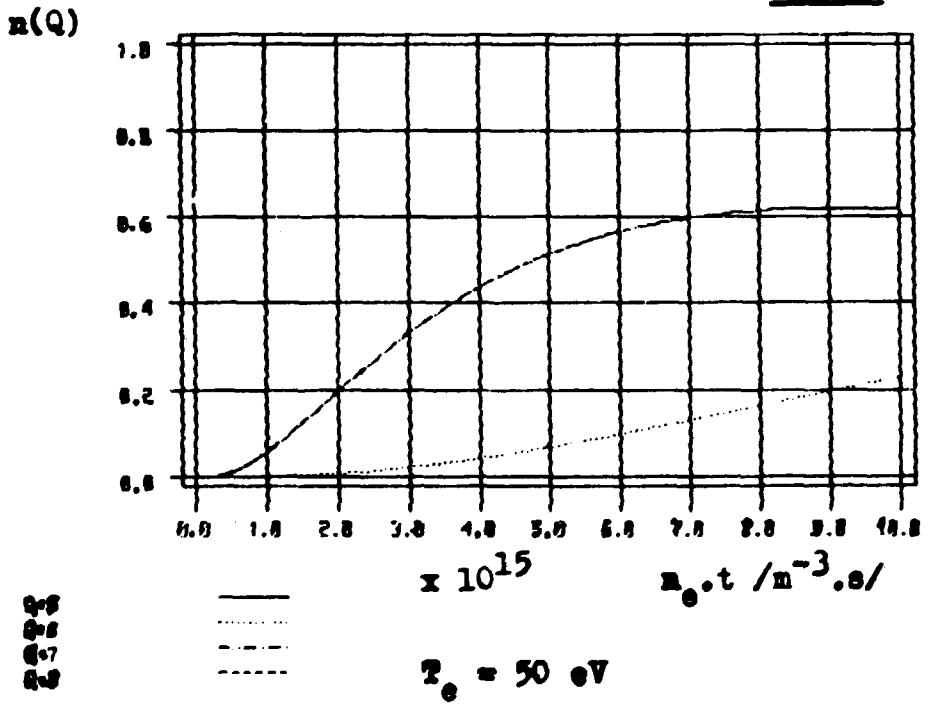

Fig.9a

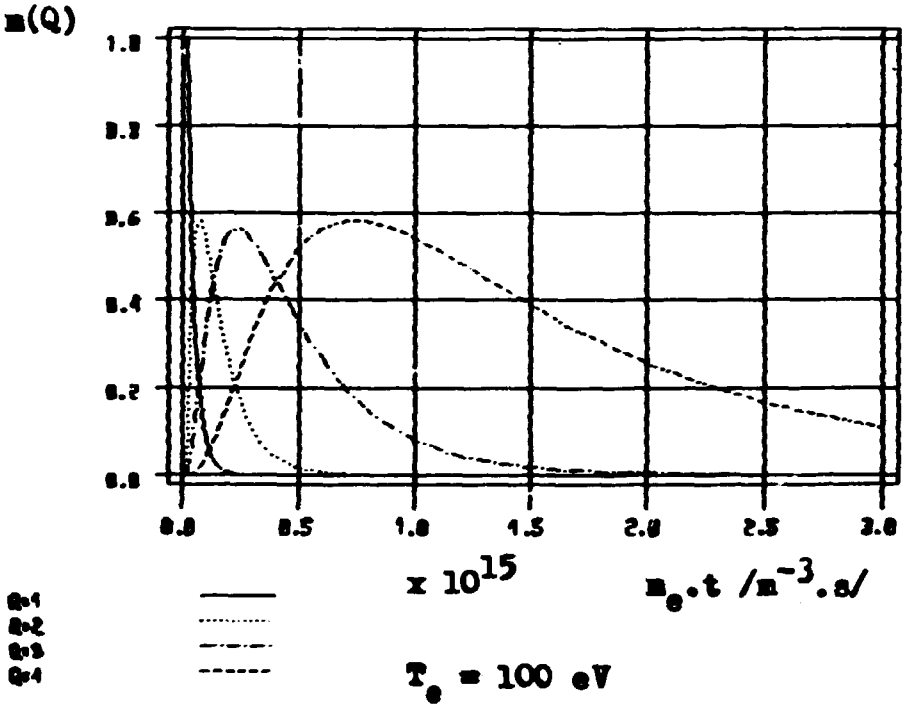
n(Q)
1.0
0.8
0.6
0.4
0.2
0.0
0.0
0.5
1.0
1.5
2.0
2.5
3.0
x 10^15
n_e.t /m^-3.s/
Q=1
Q=2
Q=3
Q=4
T_e = 100 eV

Fig.9b

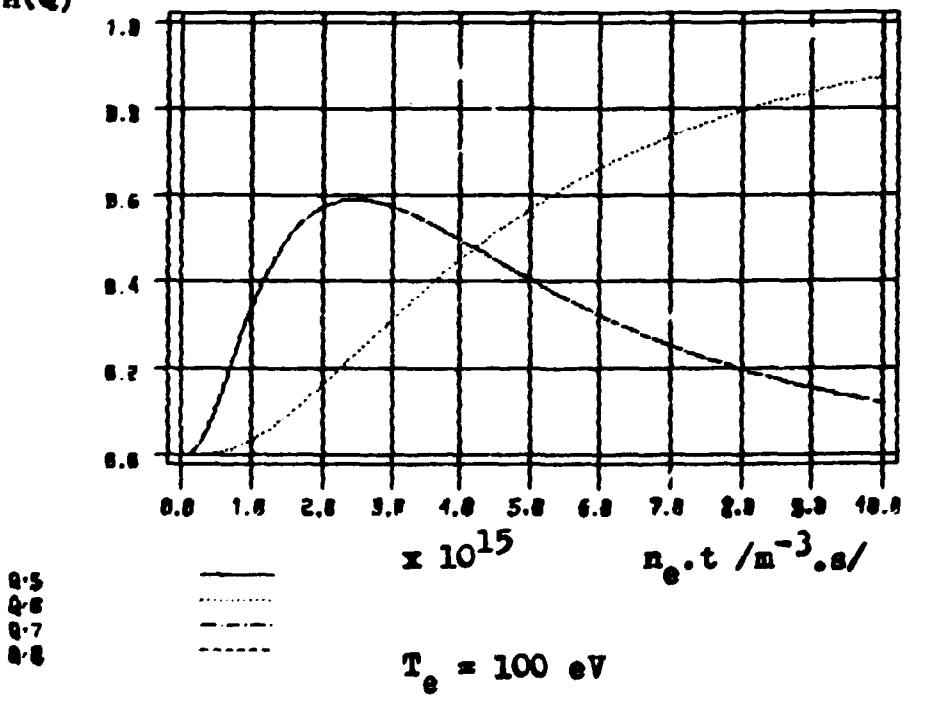
n(Q)
1.0
0.8
0.6
0.4
0.2
0.0
0.0
1.0
2.0
3.0
4.0
5.0
6.0
7.0
8.0
9.0
10.0
x 10^15
n_e.t /m^-3.s/
Q=5
Q=6
Q=7
Q=8
T_e = 100 eV

Fig.10a

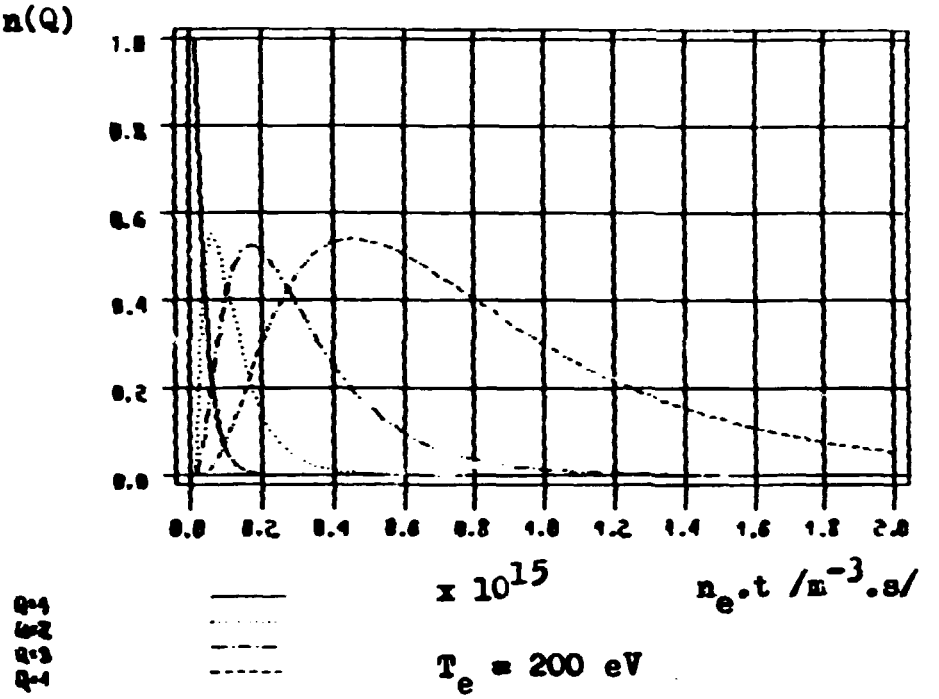

Fig.10b

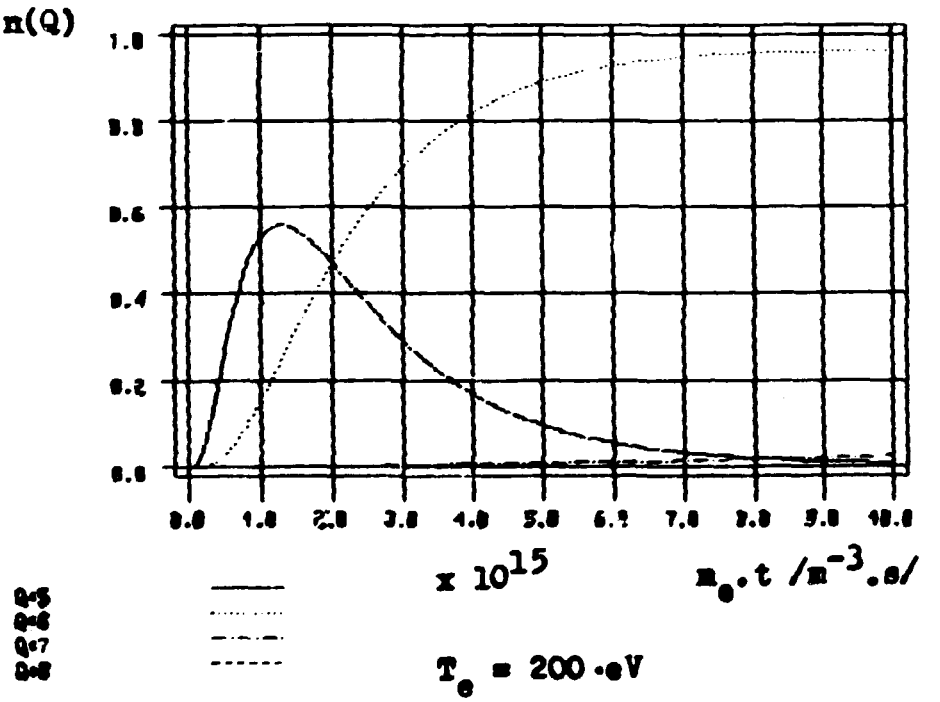

Fig.11

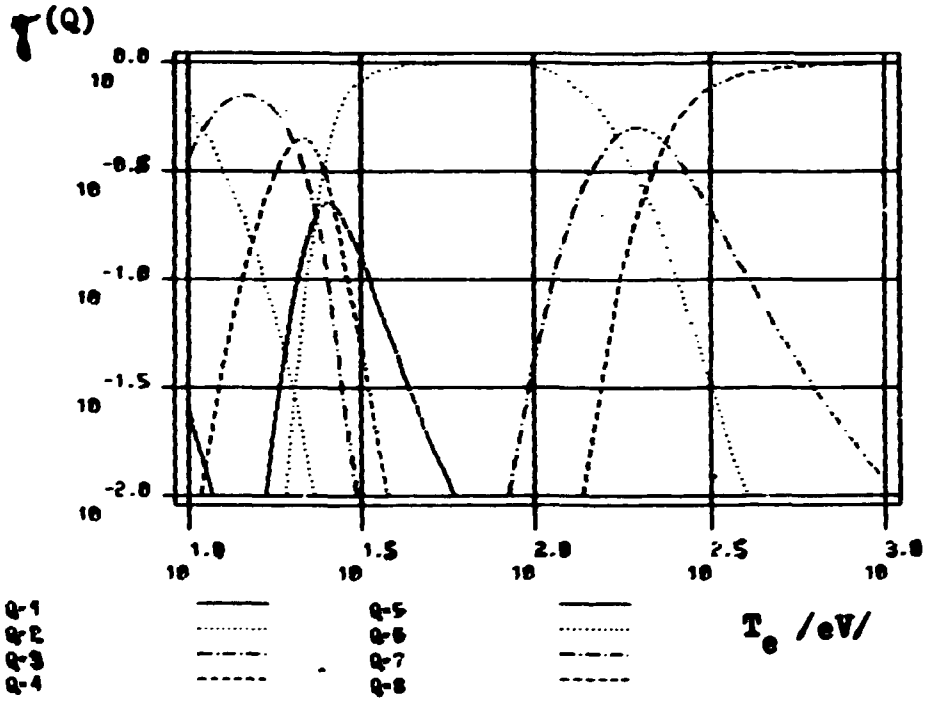
γ(Q)
0.0
10
-0.5
10
-1.0
10
-1.5
10
-2.0
10
1.0
10
1.5
10
2.0
10
2.5
10
3.0
10
Q-1
Q-2
Q-3
Q-4
Q-5
Q-6
Q-7
Q-8
T_e /eV/

Fig.12

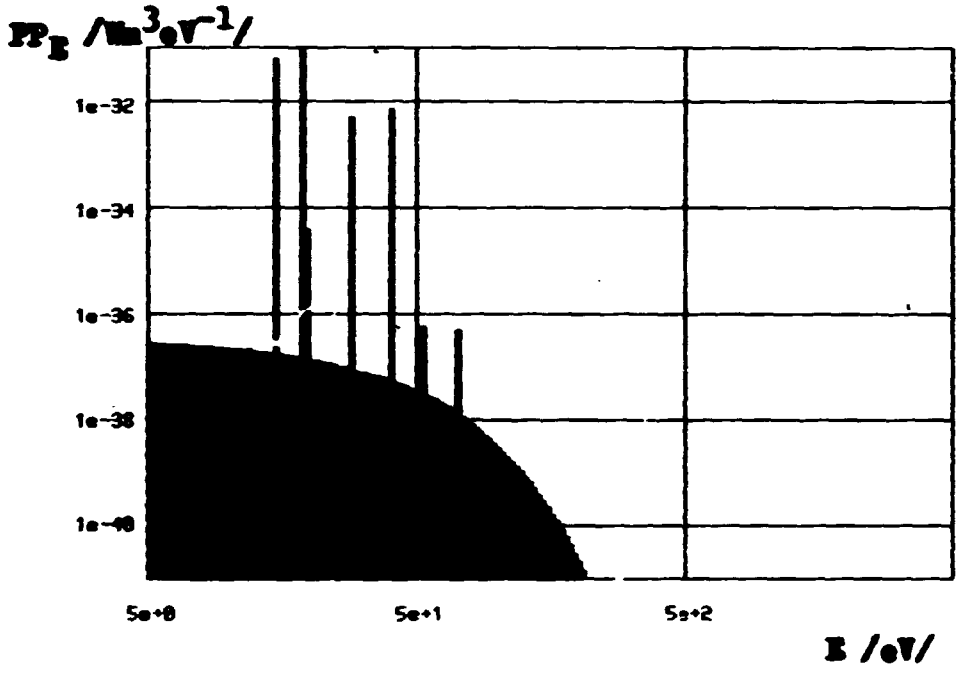

T_e = 20 eV ; $n_e.t = 2.10^{14}$ $m^{-3}.s$

Fig.13

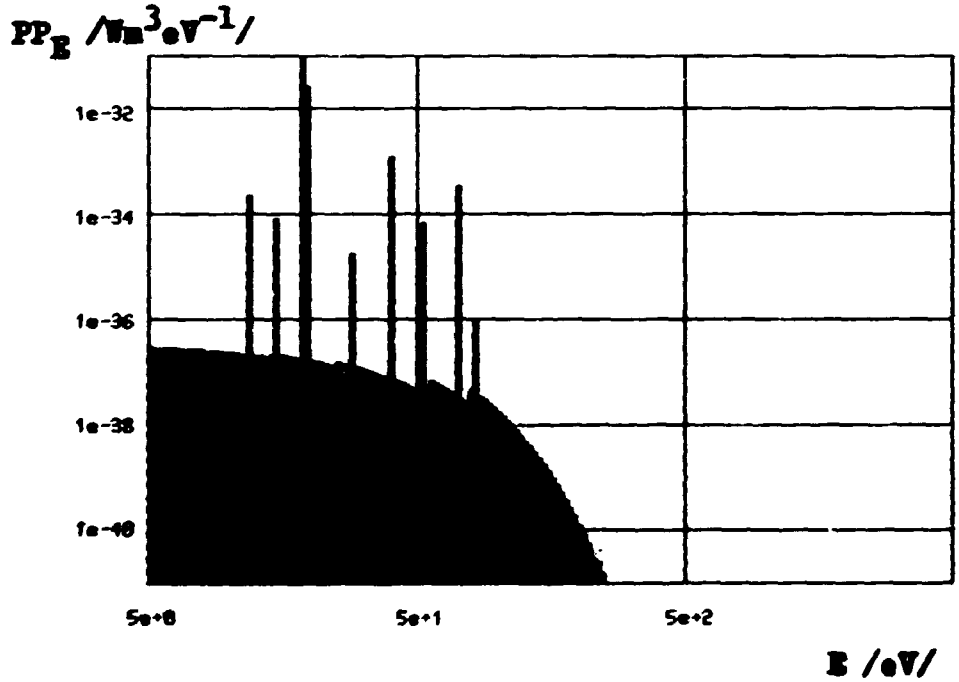

T_e = 20 eV ; $n_e.t = 5.10^{15}$ $m^{-3}.s$

Fig.14

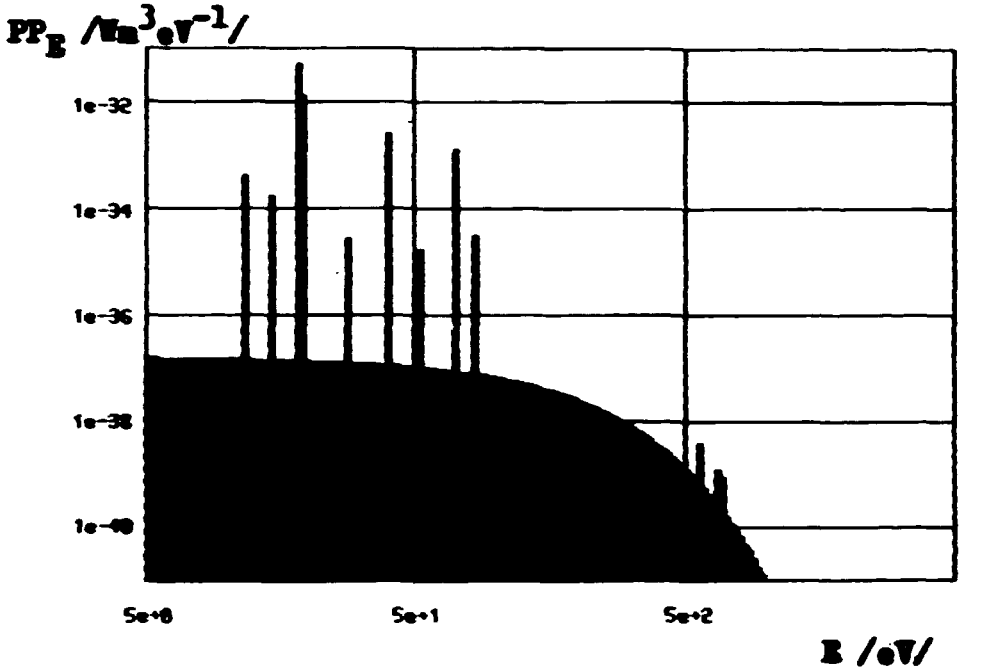

T_e = 100 eV ; $n_e.t = 2.10^{14}$ $m^{-3}.s$

Fig.15

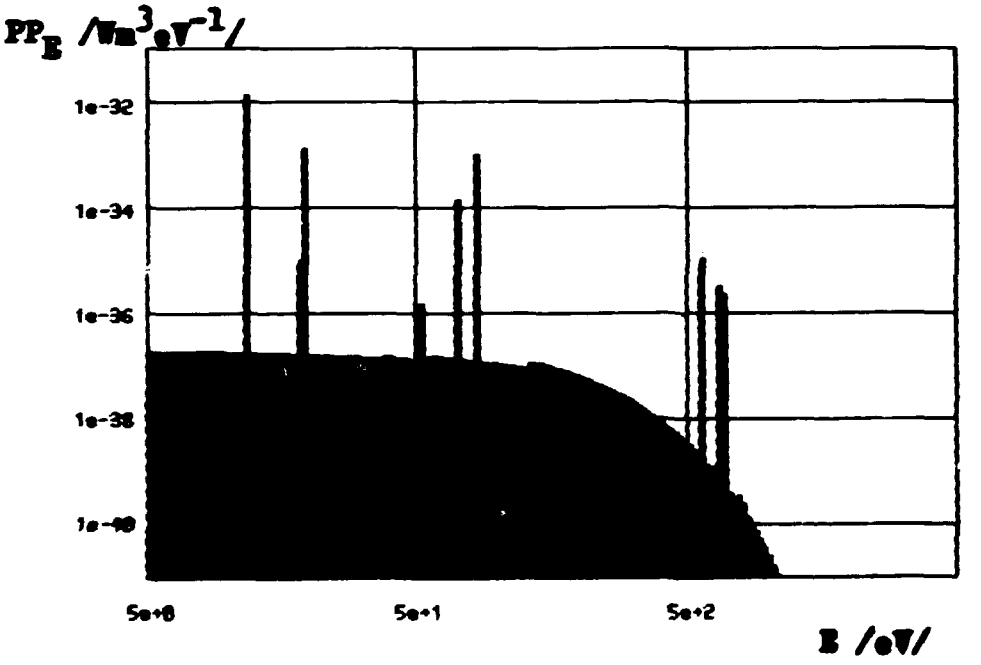

T_e = 100 eV ; $n_e.t = 5.10^{15}$ $m^{-3}.s$

Fig.16

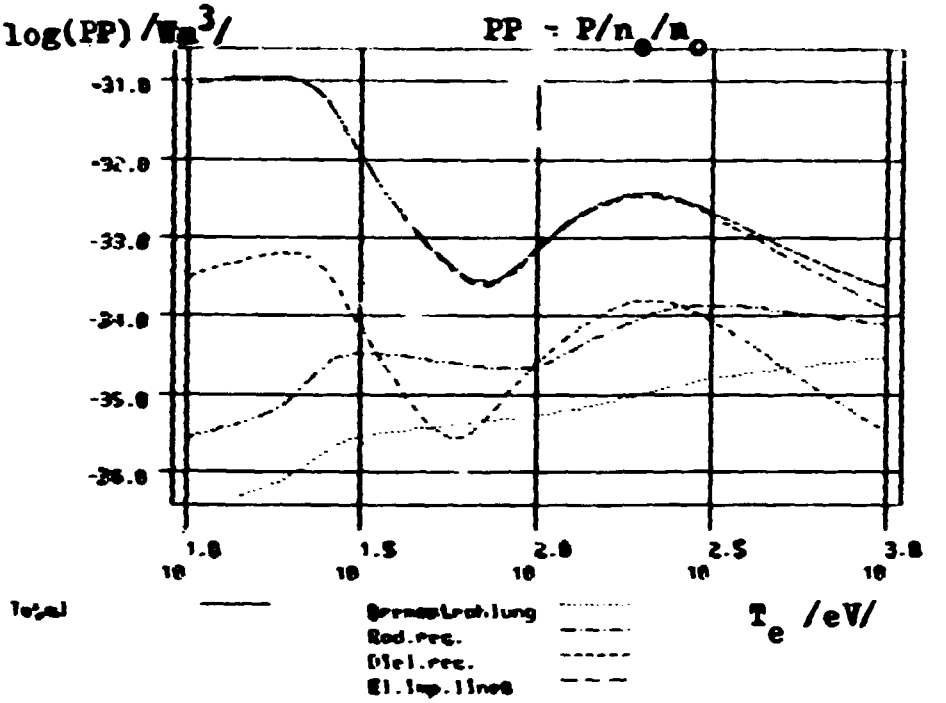
log(PP) /Wm3/
PP = P/ne/no
-31.0
-32.0
-33.0
-34.0
-35.0
-36.0
1.0 10
1.5 10
2.0 10
2.5 10
3.0 10
Te /eV/
Rad.rec.
Diel.rec.

Fig.17

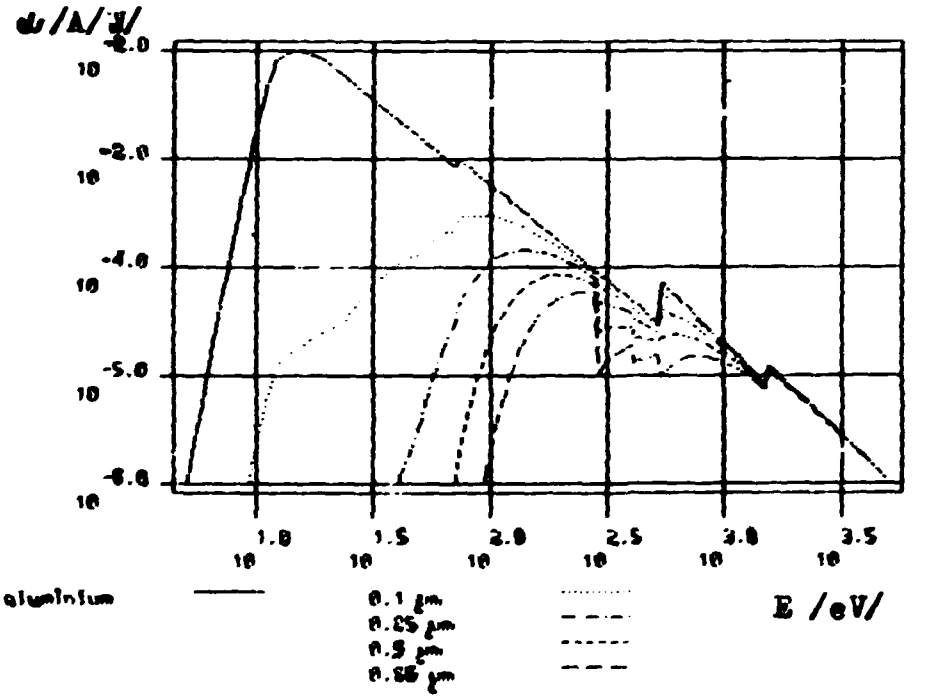
-2.0 10
-4.0 10
-5.0 10
-6.0 10
1.0 10
1.5 10
2.0 10
2.5 10
3.0 10
3.5 10
E /eV/

Fig.18a

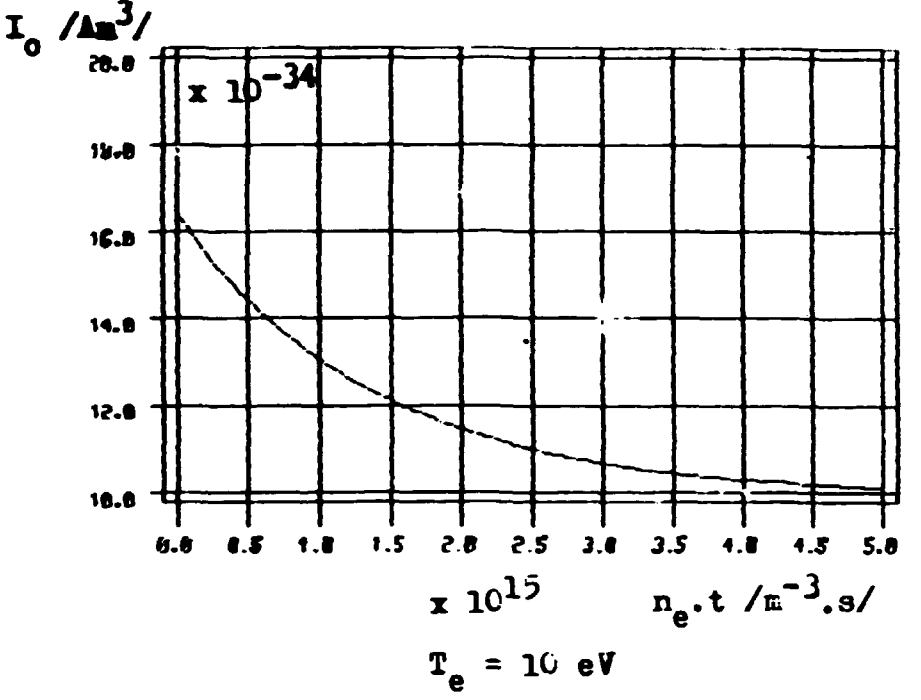

T_e = 10 eV

Fig.18b

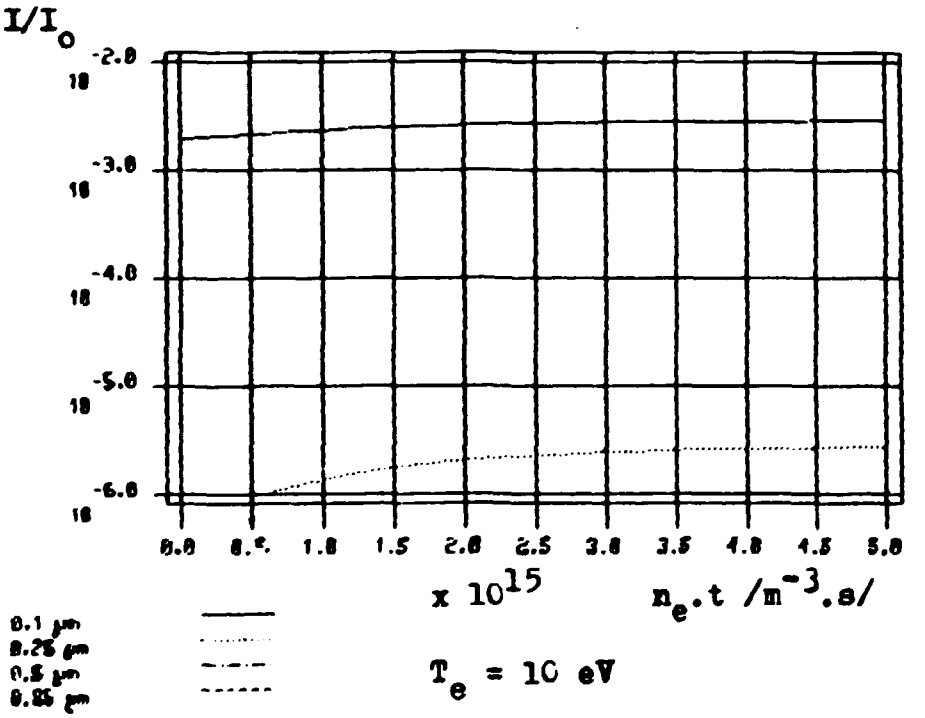

T_e = 10 eV

Fig.19a

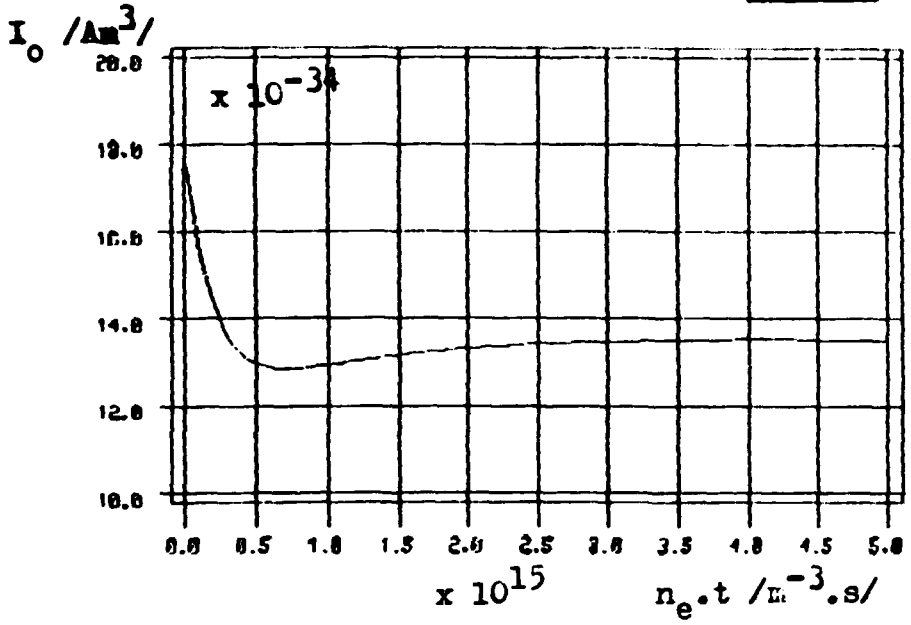

T_e = 20 eV

Fig.19b

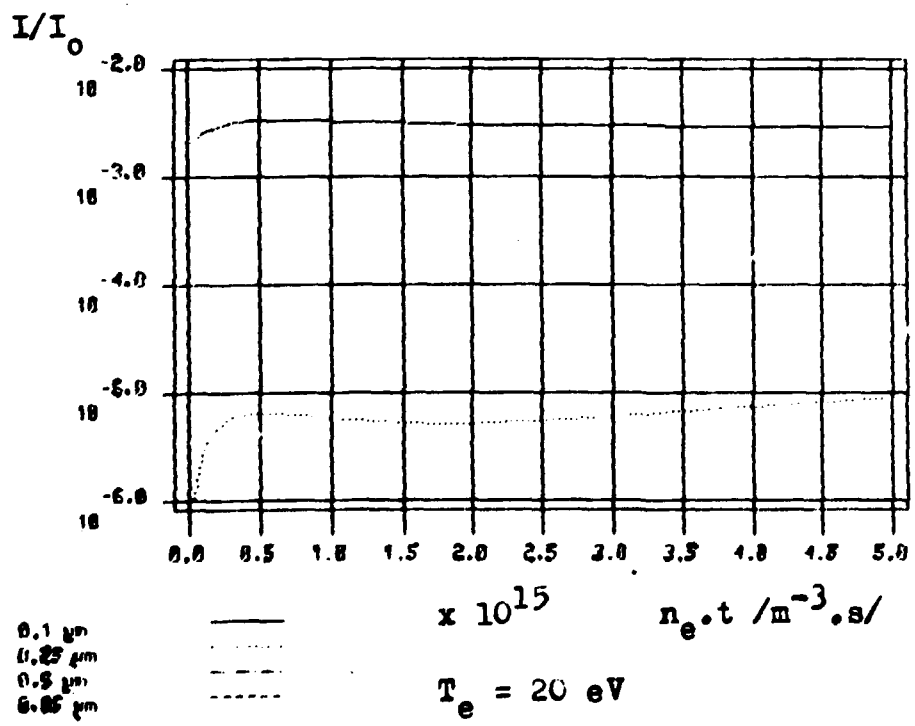

T_e = 20 eV

Fig.20a

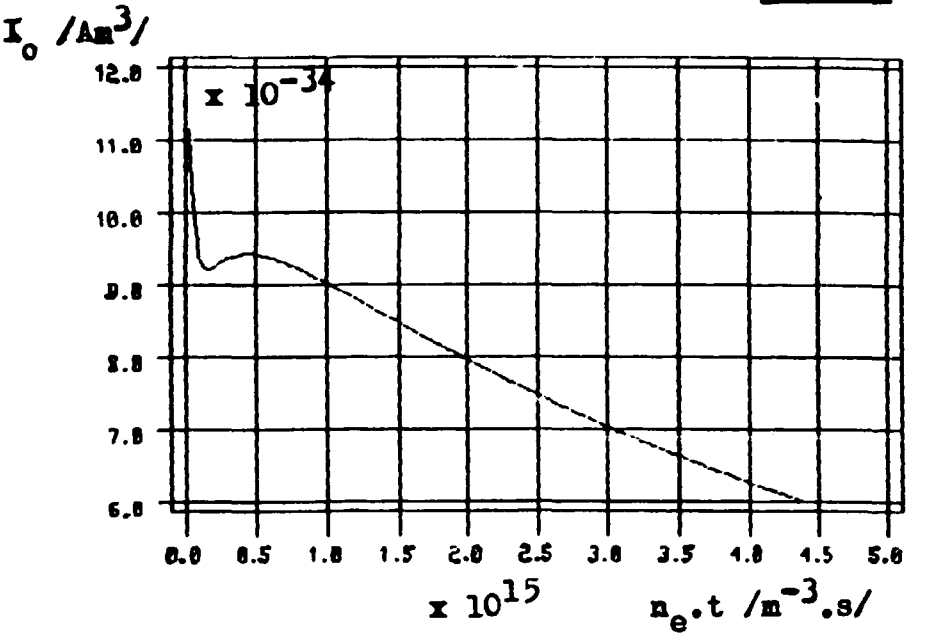

T_e = 50 eV

Fig.20b

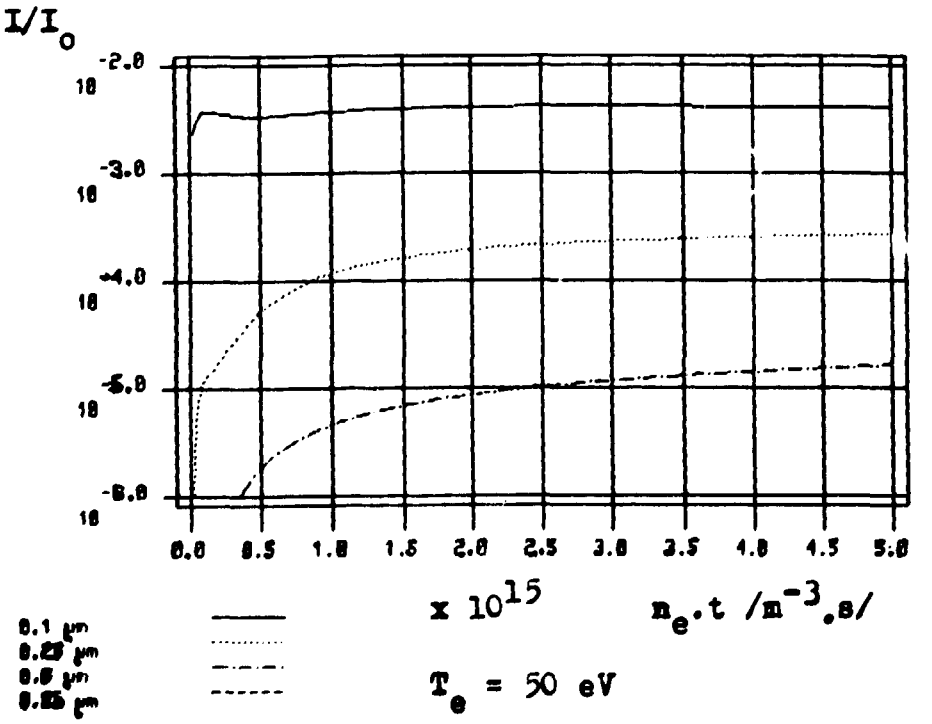

T_e = 50 eV

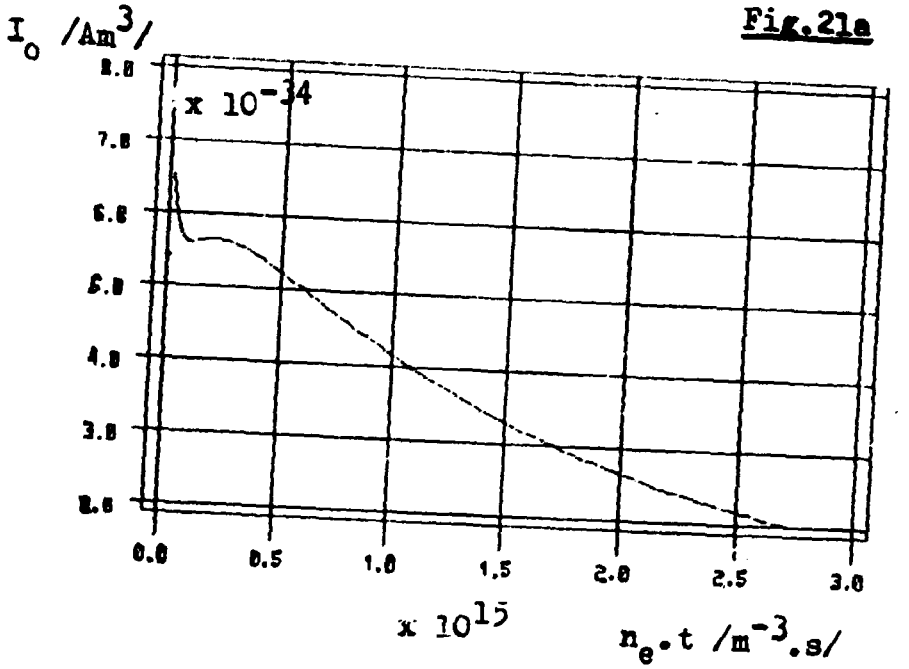

Fig.21a

T_e = 100 eV

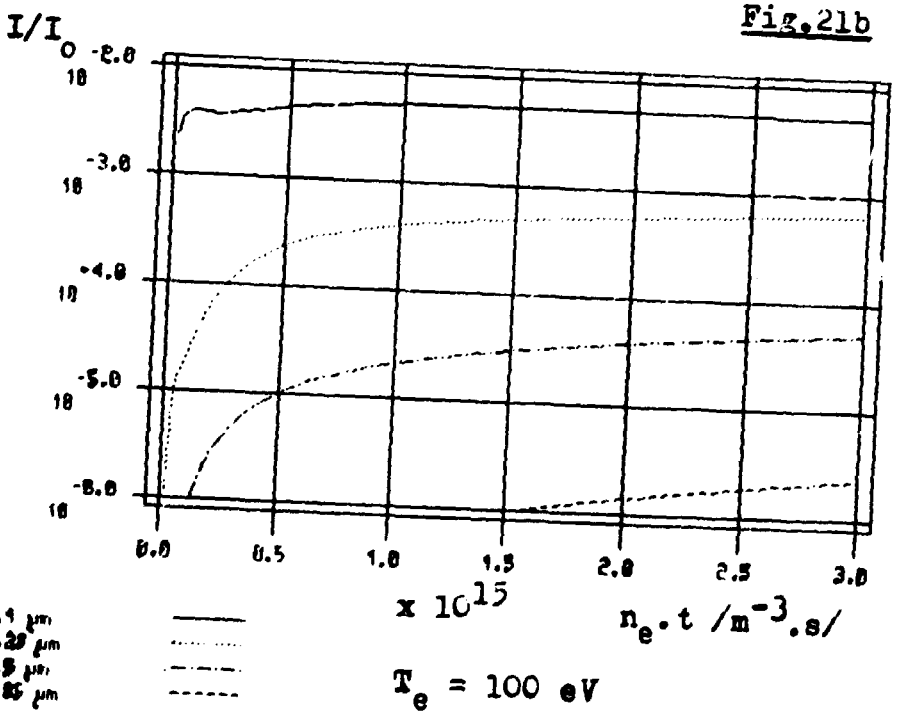

Fig.21b

T_e = 100 eV

Fig.22a

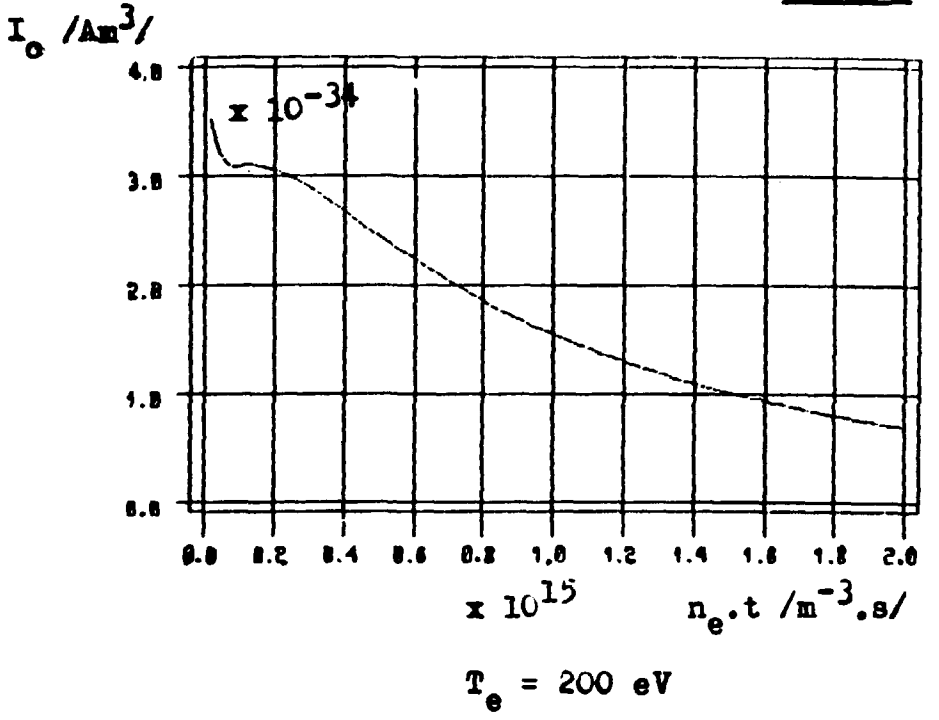

Fig.22b

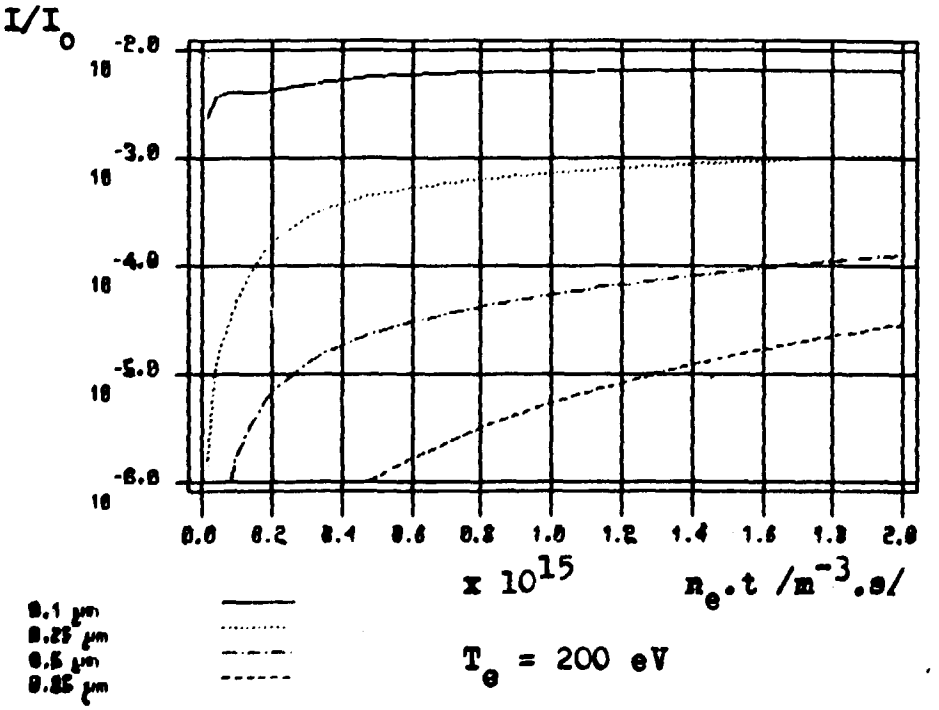

fig.23

20 dB

Fig.24

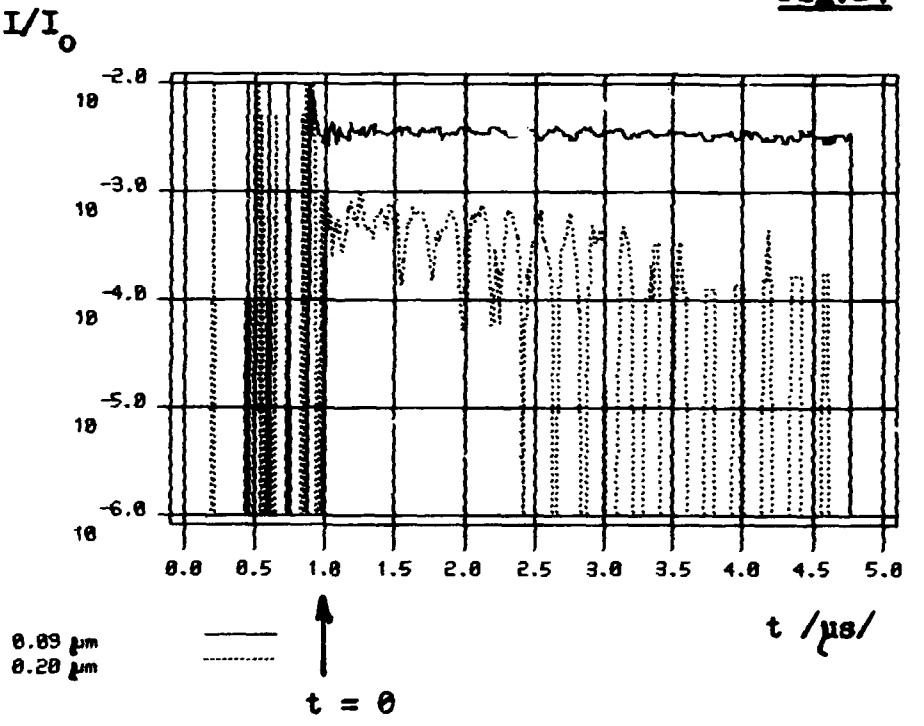
I/I0
-2.0
10
-3.0
10
-4.0
10
-5.0
10
-6.0
10
0.0 0.5 1.0 1.5 2.0 2.5 3.0 3.5 4.0 4.5 5.0
t /µs/
0.09 µm
0.20 µm
t = 0

Fig.25

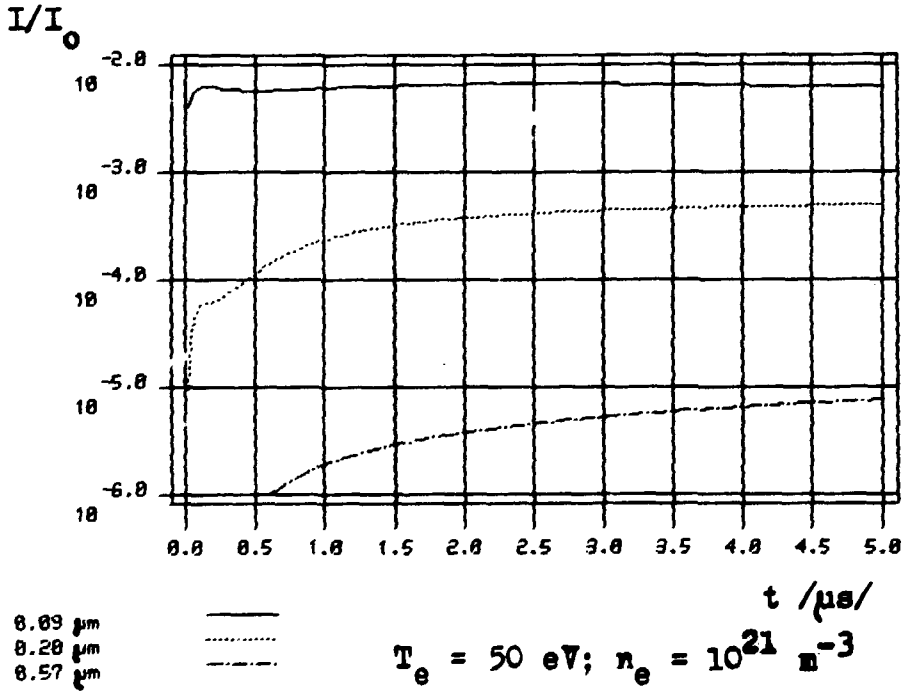
I/I0
-2.0
10
-3.0
10
-4.0
10
-5.0
10
-6.0
10
0.0 0.5 1.0 1.5 2.0 2.5 3.0 3.5 4.0 4.5 5.0
t /µs/
0.09 µm
0.20 µm
0.57 µm
Te = 50 eV; ne = 10^21 m^-3